High-frequency dielectric spectra of $AgTaO_3$-$AgNbO_3$ mixed ceramics

1995 J. Phys.: Condens. Matter 7 785

(http://iopscience.iop.org/0953-8984/7/4/009)

J. Phys.: Condens. Matter 7 (1995) 785–793. Printed in the UK

High-frequency dielectric spectra of $AgTaO_3$–$AgNbO_3$ mixed ceramics

A A Volkov†, B P Gorshunov†, G Komandin†, W Fortin‡, G E Kugel‡, A Kania§ and J Grigas‖

† Institute of General Physics, Russian Academy of Sciences, Vavilov Street 38, 117945 Moscow, Russia

‡ CLOES, University of Metz, 2 rue E Belin, 57078 Metz Cédex 3, France

§ Institute of Physics, University of Silesia, Uniwersytecka 4, 40007 Katowice, Poland

‖ Faculty of Physics, Vilnius University, Sauletekio 9, 2054 Vilnius, Lithuania

Received 8 April 1994, in final form 22 September 1994

Abstract. This paper presents the results of dielectric susceptibility investigations performed in the radiowave, microwave, submillimetre wave and infrared (IR) regions on the $AgTaO_3$–$AgNbO_3$ solid solution with Nb contents of 0.3, 0.4 and 0.6. An intense dipolar relaxation, which is responsible for the temperature dependence of the static permittivity and which freezes out at low temperatures, has been evidenced in the submillimetre wave region.

1. Introduction

The Ag compounds $AgNbO_3$ and $AgTaO_3$ belong to the oxide perovskite family ABO_3. This family exhibits a great variety of phase transitions and shows interesting fundamental and technological properties such as piezo- and pyroelectricity, ferroelectricity, optical non-linearity, photorefractivity, and even, in some cases, superconductivity [1]. At high temperatures ($T > 852$ K), $AgNbO_3$ presents the cubic prototype symmetry (C) and undergoes, on cooling, transitions to tetragonal (T) (852 K), orthorhombic (O) (658 K), and monoclinic (M_3) (620 K), (M_2) (530 K), and (M_1) (340 K) phases [2]. The phase transition sequence of $AgTaO_3$ has been shown to be C–T–M–rhombohedral (R) with transition temperatures at 777 K, 692 K, and 663 K respectively [2]. A low-temperature phase transition (120 K) to a new phase, the symmetry of which is so far unknown, has been observed by Raman scattering measurements [3]. In both $AgNbO_3$ (below 340 K) and $AgTaO_3$ (below 180 K), a weak indication of ferroelectricity has been detected [4, 5].

The solid solution $AgTa_{1-x}Nb_xO_3$ (ATN) exhibits an interesting dependence of its physical properties such as phase transition sequence and dielectric constant on x. For example, the static dielectric permittivity ε_0 increases significantly with Nb content [6, 7]. The high values reached by ε_0 in pure $AgNbO_3$ and Nb rich ATNs have been attributed, on the basis of Raman scattering experiments, to high-frequency relaxational motions connected with the Nb ions [8, 9].

These relaxational motions, evidenced as an intense and broad temperature and concentration dependent quasielastic scattering, have been believed to be coupled to a resonant oscillator with frequency between 30 and 50 cm^{-1} depending significantly on Nb concentration [8, 9]. However, the nature of these excitations remains largely debatable if only based on inelastic light scattering measurements.

0953-8984/95/040785+09$19.50

In this paper we report the results of a direct confirmation of these relaxations by dielectric studies for radiofrequencies and microwaves (1 MHz–100 GHz), submillimetre waves (150–600 GHz), and in the infrared (IR) region (100–1000 cm^{-1}).

2. Experimental conditions

The measurements were performed on $AgTa_{1-x}Nb_xO_3$ (ATN) ceramics samples with $x = 0.3$, 0.4, and 0.6. In order to cover the whole frequency range from 1 MHz to 1000 cm^{-1}, four different and complementary experimental techniques were needed. In the megahertz frequency range, the complex dielectric permittivity $\varepsilon^* = \varepsilon' - i\varepsilon''$ was obtained on Ag electrode coated plates and using a computer controlled capacitance bridge. In the frequency range from 10 MHz to 1.2 GHz and in the millimetre wave region, the measurements were performed on a coaxial and waveguide dielectric spectrometer respectively [10, 11].

Our measurements evidenced that, for the various ATN ceramics studied, the most interesting region was the submillimetre wave one from 8 to 23 cm^{-1}. For these investigations, the samples were polished plane parallel high-density ceramics of 10 mm diameter and of 20–100 μm thickness. A backward wave oscillator was placed in a quasioptical spectrometer built up in the laboratory at Moscow and including a two-beam polarizing Mach–Zehnder interferometer. With such equipment, the real ε' and imaginary ε'' parts of the complex permittivity can be determined from measurements under normal incidence of the transmission $T(\nu)$ and the phase shift $\phi(\nu)$ introduced by the ATN plates and on the basis of Fresnel's equation.

In the IR frequency region from 30 to 1000 cm^{-1}, the reflectivity spectrum was recorded with an FTIR reflection Bruker IFS 113 spectrometer on 1 mm thick polished plates. The complex permittivity was deduced by means of a Kramers–Kronig analysis, yielding a determination of ε' and ε'' with an accuracy of 10%.

All the data obtained in our investigation were determined at fixed temperature by sweeping the frequency.

3. Experimental results and discussion

Figure 1 represents the temperature dependence of the dielectric permittivity of the ATN ceramic samples measured at 1 MHz for various Nb concentrations. According to a comparison with the phase diagram deduced from x-ray structural investigations [2], the diffuse broad maximum of ε' located between 200 K and 550 K can be related to the phase transition between the two monoclinic (M_2 and M_3) phases, which almost occurs in samples with x higher than 0.2. The sharp maximum at higher temperature is attributed to the phase transition from the M_3 to the O phase.

Our first series of experiments indicated that the values of the dielectric permittivity stay nearly constant in the frequency range from 1 MHz to 100 GHz. The losses can be considered to be negligible up to 30 GHz and then slightly increase with increasing frequency above 30 GHz. This shows that the fundamental dispersion, which can be of either resonant or relaxational nature and which is responsible for the high magnitude of the dielectric permittivity, occurs at frequencies above 100 GHz.

Figures 2 and 3 exhibit dielectric spectra recorded between 1 and 20 cm^{-1} on the two ATN ceramics with $x = 0.4$ and 0.6 respectively and for various temperatures (5 K, 100 K, 250 K, 375 K, and 575 K). In figure 2, the small dots correspond to data obtained by

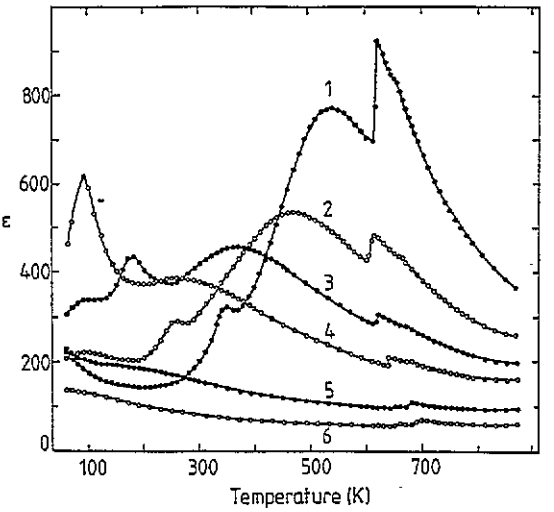

Figure 1. The temperature dependence of the dielectric permittivity of $AgTa_{1-x}Nb_xO_3$ ceramics at a frequency of 1 MHz: curve 1, $x = 1$; curve 2, $x = 0.8$; curve 3, $x = 0.6$; curve 4, $x = 0.4$; curve 5, $x = 0.2$; curve 6, $x = 0$.

the double-interferometer technique and the large dots to data deduced in the transparency region where ε' and ε'' can be calculated from the resonant transmission. The solid lines in figure 3 represent the mean values of several experimental points. Figure 4 represents a comparison at room temperature of the dielectric dispersion for the three different Nb contents investigated. In both figures 3 and 4 the points in the low-energy region from 0 to 2 cm^{-1} correspond to the microwave and 1 MHz measurements.

The IR reflectivity spectrum recorded on the ATN ceramics with $x_{Nb} = 0.6$ is reported in figure 5. The spectrum consists of at least four main vibrational modes and stays almost flat below 30 cm^{-1}, which hides clear information on the dielectric dispersion in this frequency range.

The experimental results reported in figures 2–4 reveal that in the ATN samples the main dielectric dispersion takes place in the millimetre and submillimetre wave region with a high value of permittivity and a significant rise of losses with increasing frequency. Furthermore, since the temperature dependence of the permittivity below the dispersion corresponds exactly to that of the static one, we have a clear indication for the absence of any dispersion at lower frequency.

Figures 2–4 show qualitatively that a temperature dependent excitation is strongly active at frequencies in the submillimetre range; this excitation, which has been interpreted as a relaxator [9], was also at the origin of the intense central peak detected in the Raman spectra. Furthermore in our case, it is not excluded that the spectra of $\varepsilon'(\nu)$ and $\varepsilon''(\nu)$ include contributions of the higher-frequency modes observed in the IR spectrum. In order to have an evaluation of such eventual contributions and to subtract them from the submillimetre spectrum, a dispersion analysis of the IR reflectivity spectrum of ATN was performed with a four-classical-uncoupled-oscillator model. The parameters of the model are listed in table 1, and the corresponding spectra of ε' and ε'' are reported in figure 6.

As expected, the contribution of the IR oscillators (solid lines) explains only partially the measured values of ε' and ε'' in the concerned frequency range. The difference between the experimental values of ε' and ε'' and the contribution of the vibrational modes deduced

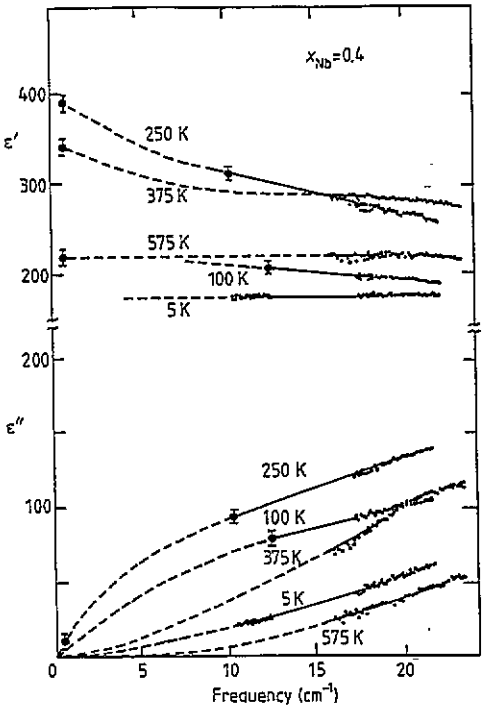

Figure 2. Submillimetre dielectric spectra of $\varepsilon'(\nu)$ and $\varepsilon''(\nu)$ of $AgNb_{0.4}Ta_{0.6}O_3$ at different temperatures. Dots and solid lines are experimental; dashed lines are extrapolations.

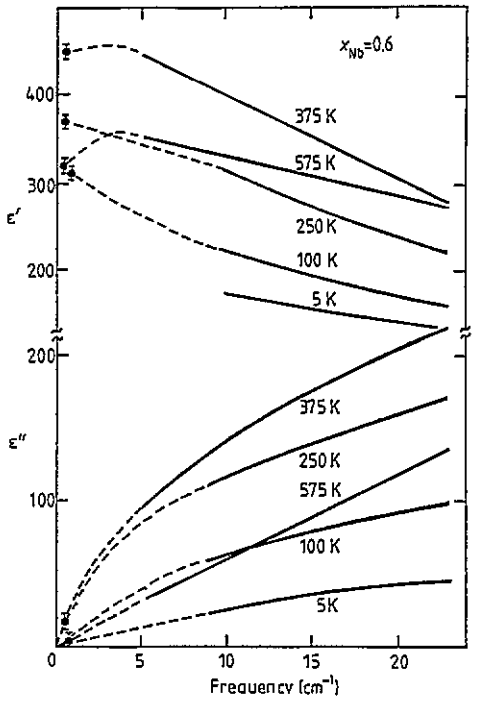

Figure 3. Submillimetre dielectric spectra of $\varepsilon'(\nu)$ and $\varepsilon''(\nu)$ of $AgNb_{0.6}Ta_{0.4}O_3$ at different temperatures. Solid lines are experimental; dashed lines are extrapolations.

from the IR reflectivity spectrum can be attributed to the high-frequency relaxator active as a central peak in the Raman spectrum.

An accurate description of the complete dielectric spectrum of ATN can be achieved by adding to the contribution of the four IR modes that due to the relaxation revealed in the submillimetre wave range, which is represented in the imaginary part ε'' as a dashed line (figure 6). This additional excitation is described by the following relaxational dispersive relation:

$$\varepsilon^*(\nu) = \Delta\varepsilon/(1 + i2\pi\nu\tau) = f\nu_r/(\nu_r^2 + \nu^2) - if\nu/(\nu_r^2 + \nu^2)$$

where $f = \Delta\varepsilon\nu_r$ is the relaxator strength, $\nu_r = 1/(2\pi\tau)$ its characteristic frequency, and τ the relaxation time. The results of these calculations for the $AgTa_{0.4}Nb_{0.6}O_3$ sample, where the dielectric dispersion in the submillimetre wave region reveals itself most clearly are shown in figure 7. In the fit of the model to the experimental data, we supposed that the IR contribution to ε'' is exclusively caused by the low-frequency IR mode (see figure 6), the parameters of which have been supposed to be only slightly dependent on temperature.

The temperature dependences of the parameters $\Delta\varepsilon$ and ν_r obtained in our model are represented in figure 8 together with the oscillator strength f. Both $\Delta\varepsilon$ and f exhibit a behaviour similar to that developed by the static permittivity (figure 1) and the sum of the dielectric contributions of the relaxator and the IR modes exactly yields the static permittivity value (~ 500 at 375 K).

$$\varepsilon(0) = \Delta\varepsilon + \Delta\varepsilon_{IR}.$$

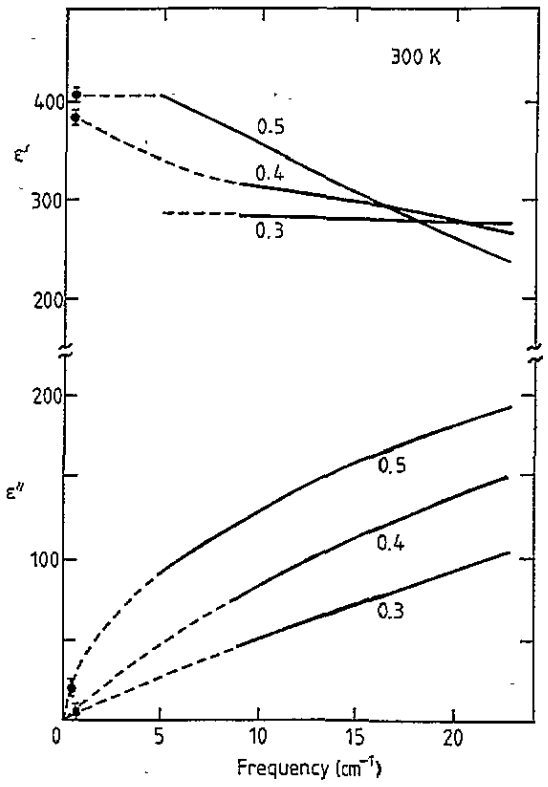

Figure 4. Submillimetre dielectric spectra of $\varepsilon'(\nu)$ and $\varepsilon''(\nu)$ of ATN of different Nb concentrations at room temperature. Solid lines are experimental; dashed lines are extrapolations.

The results obtained in the present dielectric measurements, especially those concerning the relaxation, are in good agreement with the Raman scattering data in single crystals of nearly equivalent Nb concentration. For comparison, we report in figure 9 the Raman spectrum recorded in an ATN crystal ($x \cong 0.6$), which clearly exhibits, in addition to the low-frequency phonon mode at 38 cm^{-1}, a temperature dependent central contribution reaching a maximum of diffusion near 375 K. The evaluation of this scattering was performed, similarly to the case of highly Nb doped samples [6, 8], with a scattering response function including a phonon resonator and a relaxator. The results obtained (figure 10) are comparable to those yielded in the previous submillimetre and IR investigation (figure 8). Since its characteristics strongly depend on the concentration of Nb ions, the relaxator, confirmed in our measurements, can be considered as a critical high-frequency relaxation motion [12] related to the Nb ions and certainly to off-centred motions of these ions.

These high-frequency relaxational motions for samples with high Nb concentration have been analysed as being coupled to the collective lowest-frequency phonon mode [6]. They were also shown to be responsible for the diffuse character of the phase transition between M_2 and M_3 phases. Furthermore since an equivalent behaviour occurs in pure $AgNbO_3$ single crystals [3], this unusual diffuse character cannot be interpreted by Nb concentration inhomogeneities but is clearly characteristic of this system and its Nb content.

In the sample analysed here ($x_{Nb} = 0.6$), the necessity of coupling the relaxational and the vibrational modes is not evident and the uncoupled model gives results coherent with the

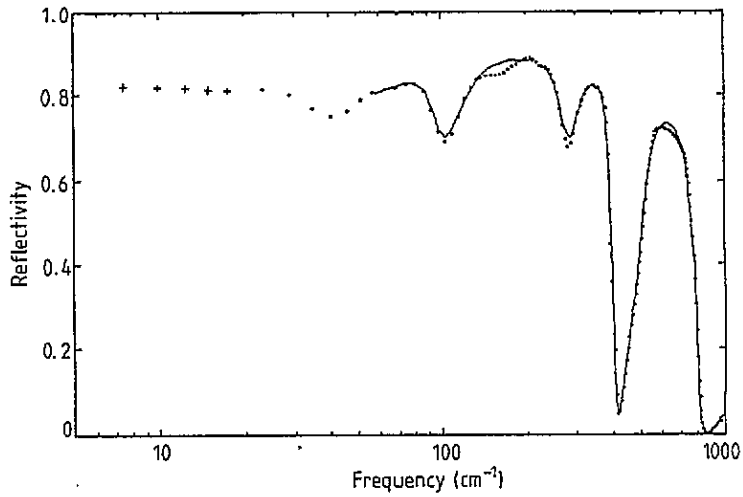

Figure 5. The IR reflectivity spectrum of $AgNb_{0.6}Ta_{0.4}O_3$ recorded at room temperature. Dots are experimental points, crosses are calculated from the submillimetre data and the solid line is a model calculation using the four-oscillator model.

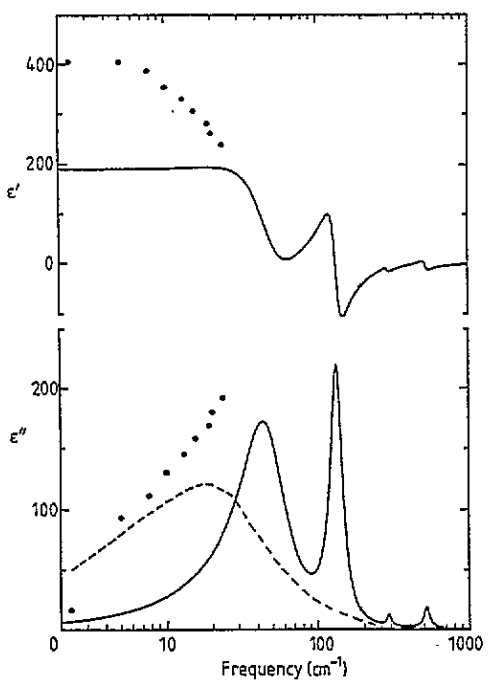

Figure 6. A comparison of the IR spectra of $\varepsilon'(\nu)$ and $\varepsilon''(\nu)$ of $AgNb_{0.6}Ta_{0.4}O_3$ (solid line) calculated from the IR reflectivity spectrum and measured submillimetre data (large dots). The dashed line shows the missing relaxator.

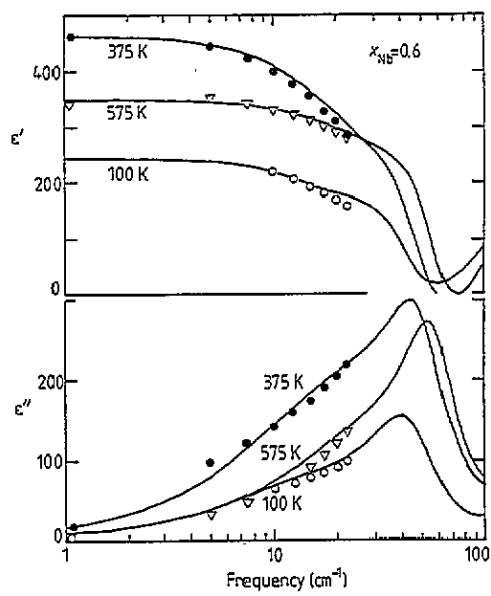

Figure 7. The dielectric dispersion in the millimetre and submillimetre wave region of $AgNb_{0.6}Ta_{0.4}O_3$ as calculated from the oscillator and relaxator additive model (solid lines) at different temperatures. Points are experimental.

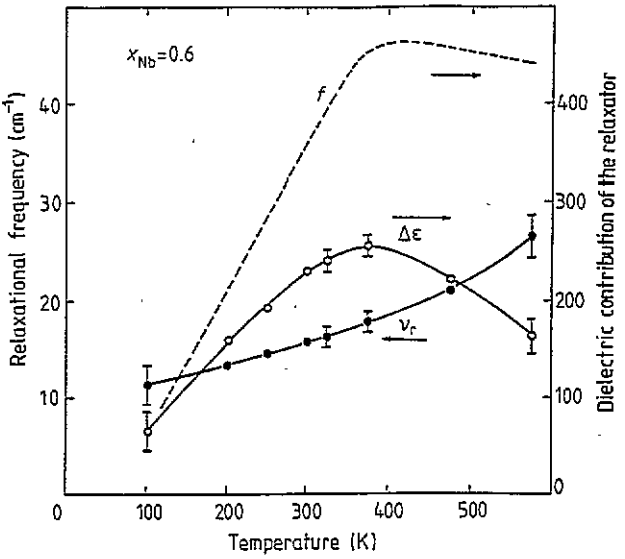

Figure 8. The temperature dependences of the parameters of the relaxator of $AgNb_{0.6}Ta_{0.4}O_3$: characteristic frequency (ν_r), dielectric contribution ($\Delta\varepsilon$), and relaxator strength (f).

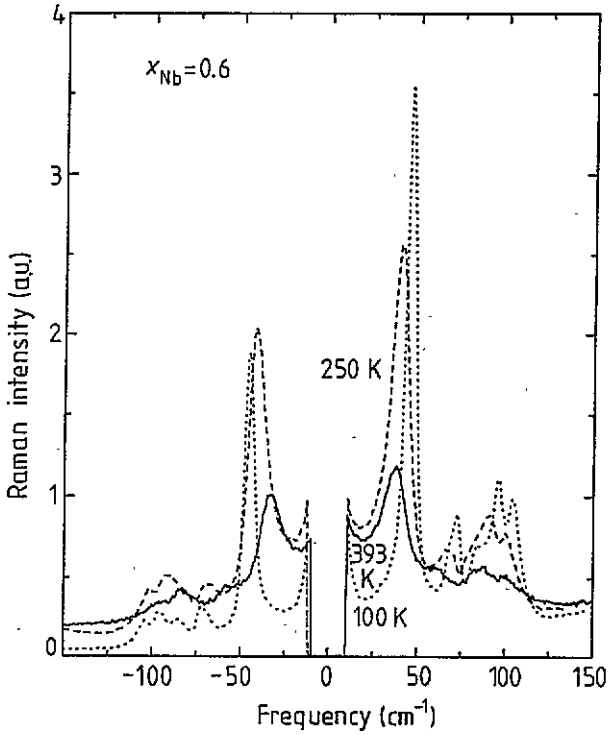

Figure 9. The low-frequency Raman spectra of $AgNb_{0.6}Ta_{0.4}O_3$ at 100, 250 and 393 K.

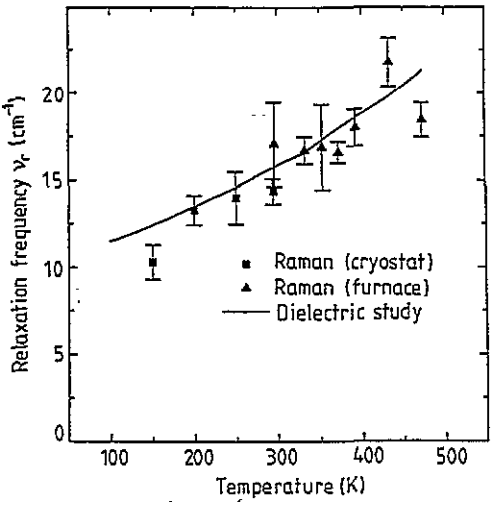

Figure 10. A comparison of the relaxation frequencies obtained by Raman spectroscopy and by dielectric investigations.

Table 1. The resonant frequency ν_0, dielectric contribution $\Delta\varepsilon$ and damping γ of the IR modes in $AgNb_{0.6}Ta_{0.4}O_3$ calculated from IR reflectivity spectra in the four-mode model.

ν_0 (cm^{-1})	$\Delta\varepsilon$	γ (cm^{-1})
47.6	139.5	41.5
134.9	47.9	30.5
291.6	0.76	22.8
518.8	1.99	57.6

submillimetre wave measurements. The validity of the coupled mode model would only be proved on the basis of further microwave measurements on samples with high Nb contents.

By comparison with other systems, the temperature dependence of the relaxational frequency observed in our system develops a rather unusual behaviour. On cooling, the critical slowing down of the polarization fluctuation (or softening of the relaxational mode) indeed occurs but not in the way characteristic of the proper order–disorder structural phase transition. The relaxational mode exhibits a gradual decrease in frequency with cooling even through the transition temperature. In contrast, the relaxator strength (dashed line) as well as $\Delta\varepsilon$ sharply decreases below the phase transition temperature, indicating a disappearance of the relaxator from the submillimetre wave region or a transformation to other degrees of freedom and a shift to other frequency ranges.

The shift of the relaxation towards lower frequencies should be observed in the dielectric spectrum as relaxation dispersion at lower temperatures. Since no relaxations have been found below 100 K in the radiofrequency and microwave regions, such an assumption has to be excluded.

4. Conclusions

Dielectric investigations in ATN solid-solution ceramics performed in the frequency range from 1 MHz to 3×10^{13} Hz have shown, in accordance with the already observed resonant

Raman modes and as confirmed by IR reflectivity, the occurrence of a strong relaxational mode in the submillimetre wave region. The temperature dependence of this motion explains the broad anomaly of the static permittivity in the vicinity of the phase transition from the M_2 monoclinic phase to the M_3 one. The behaviour of the relaxational frequency and its strength versus temperature differs from that seen in proper order–disorder or displacive ferroelectrics.

The occurrence of such a high-frequency dielectric dispersion, which constitutes the main contribution to the dielectric constant in this system and which is clearly connected to the presence of the Nb ions, on one hand, and the absence of any further lower-frequency dispersion on the other hand, obviously makes the ATN system interesting for technical device applications.

Acknowledgments

The authors are grateful to Dr J Petzelt (Prague) and Dr M Hafid (Kenitra) for useful discussions and to Dr J Banys (Vilnius) for valuable help. From the Russian side the research described in this publication was made possible in part by grant MCX 000 from the International Science Foundation and was financially supported by the Russian Foundation for Fundamental Investigations (grant 93-02/16110).

References

[1] Lines M E and Glass A M 1977 *Principles and Application of Ferroelectrics and Related Materials* (Oxford: Clarendon)
[2] Pawelczyk M 1987 *Phase Transitions* **8** 273
[3] Kugel G E, Fontana M D, Hafid M, Roleder K, Kania A and Pawelczyk M 1987 *J. Phys. C: Solid State Phys.* **20** 1217
[4] Kania A, Roleder K and Lukaszewski M 1984 *Ferroelectrics* **52** 265
[5] Kania A and Roleder K 1984 *Ferroelectr. Lett.* **2** 51
[6] Hafid M, Kugel G E, Kania A, Roleder K and Fontana M D 1992 *J. Phys.: Condens. Matter* **4** 2333
[7] Kania A 1983 *Phase Transitions* **3** 131
[8] Kania A, Roleder K, Kugel G E and Fontana M D 1986 *J. Phys. C: Solid State Phys.* **19** 9
[9] Fontana M D, Kugel G E, Kania A and Roleder K 1985 *Japan. J. Appl. Phys.* **24** *Suppl.* 24–2, 516
[10] Brilingas A, Davidovich R I, Grigas J, Lapinskas S, Medkov M, Samulionis V and Skritskij V 1986 *Phys. Status Solidi* a **96** 101
[11] Grigas J, Brilingas A and Kalesinskas V 1990 *Ferroelectrics* **107** 61